Article

Utilizing Multi-Temporal ALOS/PALSAR Backscatter Data to Detect Deforestation in the Indonesian Tropical Forest

I GD Yudha Partama [a]*, Kakuji Ogawara [b]

[a] *Regional Planning and Environmental Management Study Program, Universitas Mahasaraswati Denpasar, Denpasar, Indonesia*

[b] *Mechanical Engineering Division, Yamaguchi University, Yamaguchi, Japan*

* *Correspondence: yudhapartama@unmas.ac.id; Tel.: +62-361-256-162*

Received: 19 April 2020; Accepted: 29 November 2023; Available online: 12 March 2024

Abstract

Deforestation detection mapping has been analyzed using Synthetic Aperture Radar (SAR) data from the ALOS PALSAR satellite. SAR is a promising tool for deforestation mapping in tropical forest regions because microwave energy can penetrate clouds. This study examined the effect of SAR polarization on the accuracy of deforestation mapping and the seasonal variation of radar backscattering values in Riau Province, Indonesia. Image differencing was used to determine the threshold value for distinguishing between forest and non-forest areas. The difference between HV (horizontal transmit-vertical receive) and HH (horizontal transmit-horizontal receive) polarization was used as the discriminant variable. The correlation between radar backscattering value and accumulated rainfall was also analyzed to assess the effect of seasonal change. The findings demonstrated that the accuracy of deforestation detection mapping using HV polarization outperforms that achieved with HH polarization. Moreover, seasonal variations in rainfall were observed to influence radar backscatter signatures in bare soil, acacia, and oil palm, though no such influence was detected in forested areas. The accuracy of deforestation detection mapping, employing the thresholding method, reached a rate of 92.21%. During the period from November 2007 to July 2009, forested areas in Riau experienced a reduction, decreasing to 6.77%, and further decreasing to 6.08% by October 2010.

Keywords: *deforestation; Synthetic Aperture Radar (SAR); polarization; seasonal changing; thresholding method*

1. Introduction

The Indonesian rainforest is among the World's richest biodiversity and covers a significant area of the world's tropical deep peat. The Government of Indonesia estimates that, between 2003 and 2006, around 1.17 million Ha of forest was cleared or degraded each year (WWF Indonesia, 2008). As vast and rapid changing of forest region, direct monitoring seems impossible to be applied.

Remote sensing is viewed as an important and verifiable method for monitoring forest cover and its changes. Moreover, it provides suitable information for the objective of the United Nations Framework Convention on Climate Change (UNFCCC) Reducing Emission from Deforestation and Forest Degradation (REDD+) program. Optical remote sensing data are used in many studies to monitor tropical forest status (Hansen et al., 2008; Tsuyuki et al., 2011; Margono et al., 2012). However, optical sensors are often difficult to obtain cloud-free images in tropical regions due to frequent cloud cover and haze from the forest fire.

Meanwhile Synthetic Aperture Radar (SAR) is a future complement for forest monitoring due to the independence of cloud-cover and solar illumination because SAR is operating at microwave frequency. Advanced Land Observing Satellite (ALOS) Phased

Array L-Band Synthetic Aperture Radar (PALSAR) with longer radar wavelength L-band (23.62 cm wavelength) and finer resolution (12.5 m) is more suited to the delineation of forest cover and deforestation detection on the regional and global scale because of greater penetration through the canopy (Shimada et al., 2009).

However, deforestation detection using SAR images were influenced by several factors such as environmental conditions and SAR system characteristic (polarization and wavelength) (Kiage et al., 2005). Japanese Earth Resources Satellite-1 (JERS-1) which only using co-polarized (HH-polarization) backscatter data was found to decrease around 1.5 dB for deforested areas in the British test site (Thiel et al., 2006). Based on this research, the backscatter difference between deforested areas and natural forests using co-polarized is insignificant and difficult to distinguish between the deforested areas and natural forests. ALOS/PALSAR data provided the Fine Beam Dual Polarization (FBD) mode with HH and HV polarization. Therefore, the study to evaluate the SAR system polarization with different polarization (HH and HV polarization) using ALOS/PALSAR FBD is needed to establish a robust method for deforestation detection.

Another factor that can influence the detection of deforestation is the presence of environmental conditions at the time of image acquisition. The largest contrast (dynamic range) between mean forest backscatter and mean deforested backscatter appears in the driest season and the lowest contrast appears in the wet season (Salas et al., 2002; Whittle et al., 2012). For example, temporal and spatial variability of JERS-1 data for deforested areas in central Rondonia was explained as a consequence of rainfall events and heterogeneous soil moisture distribution (Salas et al., 2002). To reduce the errors in the interpretation of deforestation detection, evaluating the stability of the thresholding method based on the seasonal changing effect caused by rainfall events is needed.

This research was conducted to investigate forest cover loss in Riau Province using the thresholding method and aimed to examine the potential of multi-temporal ALOS PALSAR FBD data for deforestation detection mapping, assess the impact of SAR polarization on the accuracy of deforestation detection mapping, analyze the influence of seasonal changes, particularly those resulting from rainfall events, on radar backscattering signatures in tropical environmental regions, establish a method for deforestation detection and calculate the accuracy of the deforestation map using the thresholding method, and calculate the percentage of forest cover loss in the Riau study area using the thresholding method.

2. Methods

2.1 Research study area

The research locations are located in Riau Province on Sumatra Island and South Borneo, Indonesia as shown in Figure 1. Based on Global Forest Watch (GFW) data, the most intense deforestation occur on these sites.

Figure 1. Study Area

2.2 Data collection

The data in this research are as follows; ALOS/PALSAR FBD 12,5 m line spacing data (from 2007-2010) obtained from Japan Aerospace Exploration Agency (JAXA) at processing level 1.5, secondary data of ground truth point taken from WWF (World Wild Found) Indonesia and Google Earth (GE), rainfall data taken from Daily Global Satellite Mapping of Precipitation (GSMap), and the tree cover loss from Global Forest Watch (GFW).

2.3 Data analysis method

The research process is divided into two parts, research framework 1 shows the flow chart of evaluation of the influence of SAR polarization (HH&HV) and seasonal changing on the accuracy rate by using the thresholding method. The thresholding method was used to determine the threshold value of σ^0difference from an image before and after deforestation events by calculating the DR, FAR, and AR. The confusion matrix was used to assess the accuracy of the deforestation map, and then the forest cover loss areas can be calculated.

Research framework 2 shows the flow chart of evaluation of the influence of seasonal changing on the radar backscattering value. In the first step, DN of ALOS/PALSAR level 1.5 was converted to NRCS in dB. The next step is extracting the region of interest (ROI) for each LU/LC from NRCS images based on the ground truth point from secondary data (WWF & GE). Analysis of the correlation between 10-days of accumulated rainfall and NRCS was conducted to get the coefficient of determination (R2) from this relationship.

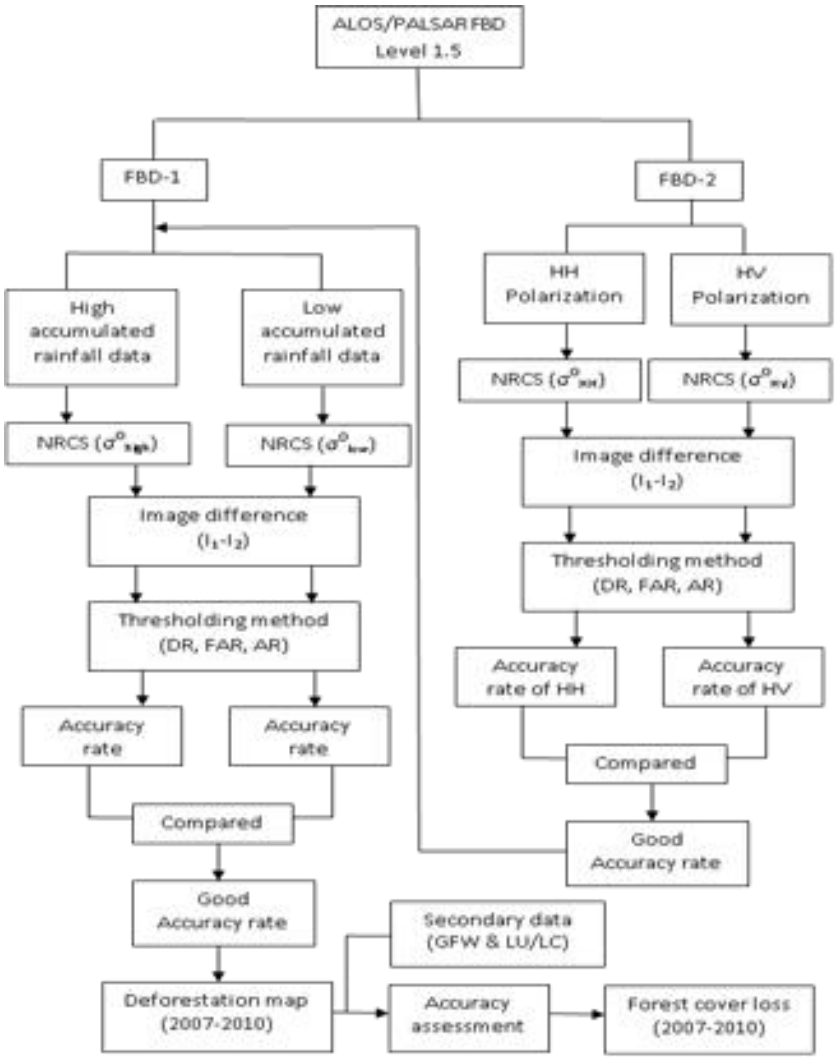

Figure 2. Research Framework 1

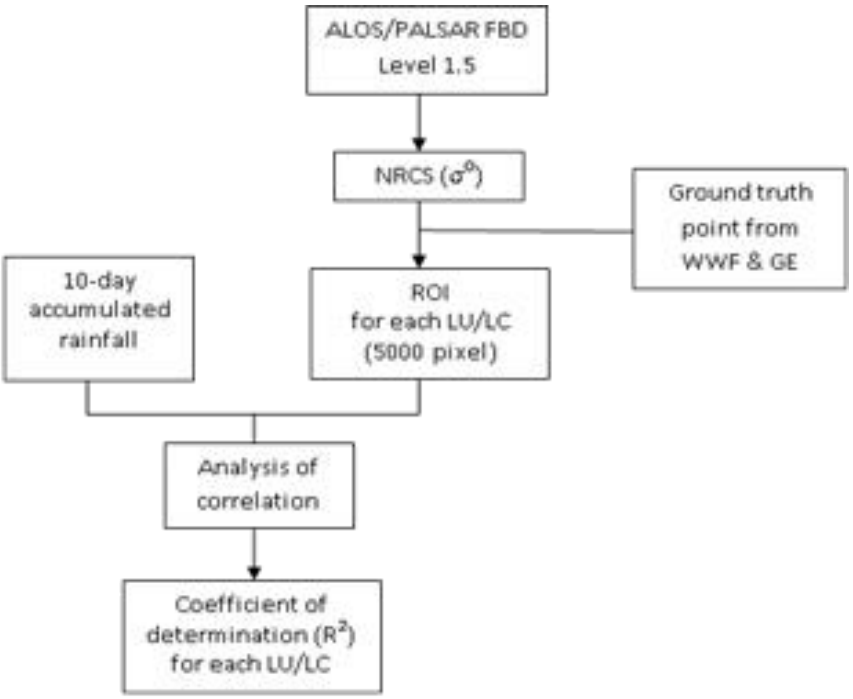

Figure 3. Research Framework 2

2.4 Data Processing

2.4.1. Pre-processing of the time series of PALSAR FBD data

The multi-temporal PALSAR FBD 1.5 level data were filtered using a Low Pass filter with a 3x3 window size to reduce the speckle and noise. The Digital Number (DN) values (amplitude values) were converted into Normalized Radar Cross Section (NRCS) in decibel (dB) unit according to the formula from JAXA and the parameters from the metadata of each file:

$$\sigma^0[dB] = 10\ x\ log10\ (DN)^2 + CF(Shimada,\ 2009) \quad (1)$$

Where σ^0 is the backscattering coefficient, DN is the digital number value of pixels in HH or HV and CF is the absolute calibration factor of -83.

2.5 Data analysis

2.5.1. Change detection method for deforestation mapping

a. Image Differencing

In this technique, PALSAR images of the same area after being converted to σ^0 intensity, obtained from time t1 (after deforested) and t2 (before deforested), were subtracted pixel-wise. Mathematically, the different image is

$$\sigma^0{}_d(x, y) = \sigma^0{}_1(x, y) - \sigma^0{}_2(x, y) \quad (2)$$

Where, $\sigma^0 1$ and $\sigma^0 2$ are the images obtained from t1 and t2, and (x,y) are the coordinates of the pixels. The resulting images, $\sigma^0 d$ represent the backscatter intensity difference of $\sigma^0 1$ and $\sigma^0 2$.

b. Evaluation of thresholding method for deforestation detection

The detection rate (DR), false alarm rate (FAR), and accuracy rate (AR) was calculated to evaluate the accuracy of threshold detection. The detection rate is defined as the probability if a pixel is detected as "deforested" by PALSAR (DFPALSAR) when it is

"deforested" by reference data (DFreference). The detection rate is estimated as (Motohka et al., 2014):

$$DR = P(DF_{PALSAR} | DF_{reference}) \quad (3)$$

The false alarm rate is defined as the probability if a pixel is detected as "deforested" by PALSAR (DFPALSAR) when it is "Un-disturb forest" by reference data (UFreference). The false alarm rate is estimated as

$$FAR = P(DF_{PALSAR} | UF_{reference}) \quad (4)$$

The accuracy rate (AR) is total correct detection (deforested area and un-disturb forest; Ncorrect) divided by the total number of pixels (Ntotal). The accuracy rate is estimated as

$$AR = N_{correct} / N_{total} \quad (5)$$

2.5.2. Evaluation of HH and HV polarization to detect the deforestation

The FBD images (HH and HV) were selected to evaluate the ability both of polarization to detect deforestation in deforested areas using PALSAR images acquired in 2007 and 2009. The Region of Interest (ROIs) was selected in deforested areas and natural forests according to reference data from Global Forest Watch data and Land use/cover. The total pixel selected is 5000 pixels for each land cover. The selected points were used for the evaluation of a thresholding method using the above method to discriminate the deforested areas and the accuracy rate of polarization. The polarization which has a good accuracy rate will be selected for the following analysis.

2.5.3. Evaluation of seasonal variation on radar backscattering coefficient (σ^0)

Analysis correlation between σ^0 for each land cover and 10-day accumulated rainfall data was performed to investigate the influence of ground surface moisture on radar backscattering intensity. The 10-day accumulated precipitation was calculated before the PALSAR observation date for each reference point as a possible indicator of the ground surface moisture condition.

2.5.4. Evaluation of seasonal variation's effect on deforestation detection

The multi-temporal PALSAR FBD images from 2007-2010 were selected to evaluate the seasonal changing effect on the accuracy of deforestation mapping. The FBD image acquired in 2007 are used as a standard for calculations ($\sigma^0$2) and we selected the time-series images from 2009-2010 ($\sigma^0$1) to compare the difference in the accuracy of deforestation detection between high and low accumulated precipitation data.

2.6 Deforestation mapping

The last is calculating the σ^0 difference between the input and base images. Non-forest areas were masked using the forest/non-forest map. Deforestation mapping results were obtained by applying a threshold determined by the above-mentioned analysis for multi-temporal σ^0 difference. The deforestation map from each year was combined to make the final deforestation map (November 2007 to October 2010). The accuracy of the deforestation map was evaluated by using the confusion matrix method.

3. Results and Discussion

3.1 Evaluation of HH and HV polarization to detect the deforestation

Figure 4 shows the temporal average of σ^0HH. There are no clear changes after deforestation events, but the temporal average of σ^0HV is systematically decreased by 3-5 dB after deforestation events.

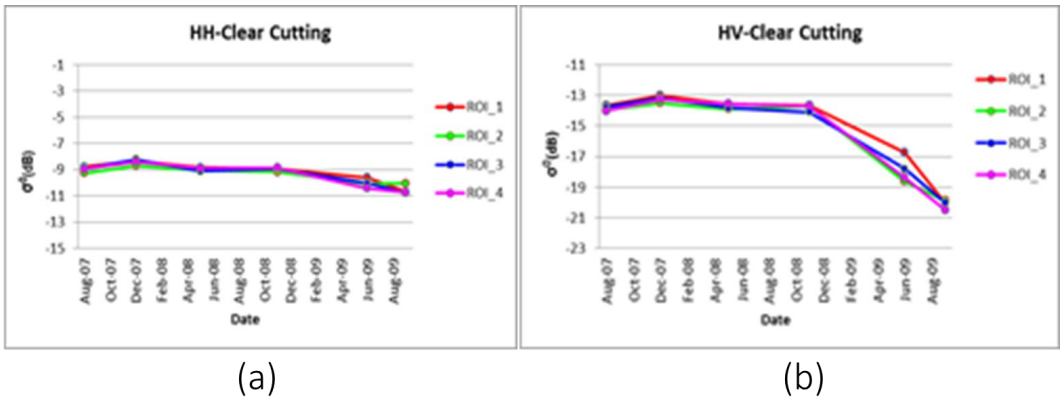

Figure 4. Characteristic of backscatter value (σ^0) for HH polarization (a) and HV polarization (b) during deforestation events, (ROI: Region of Interest)

Figure 5 illustrates the detection rate, false alarm rate, and accuracy rate of deforestation detection obtained by using various thresholds for HH and HV polarization. The false alarm rate of both polarization shows similar behavior, it rapidly increases at a threshold around -2 dB. While the detection rate rapidly grows at a threshold around – 5 for HH and -7 for HV. The accuracy rate of deforestation detection for HH is significantly smaller than HV polarization. The maximum accuracy rate of HH and HV were 77% and 94.8% respectively when threshold values are -1 and -2.5 dB.

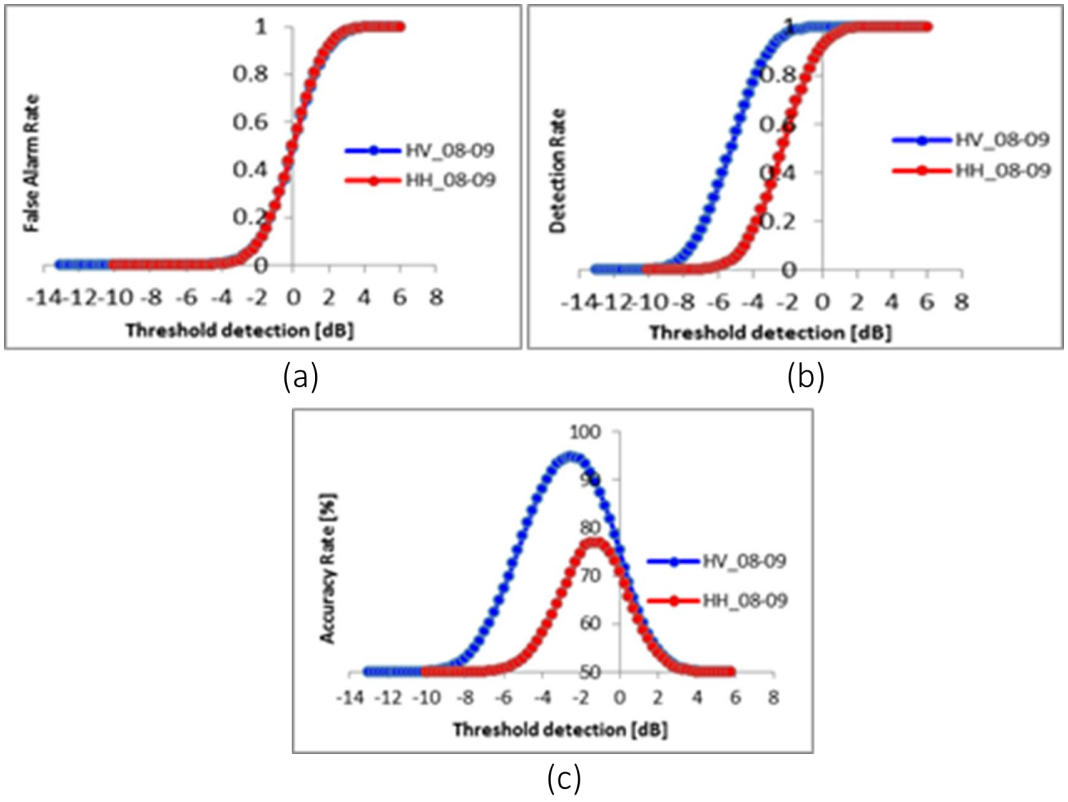

Figure 5. (a) False alarm rate, (b) detection rate, and, (c) accuracy rate for HH and HV polarization

Figure 6 shows the histogram of difference σ^0 for deforested and forest no change areas. For the HH polarization image, the number of pixels overlapping between deforested and forest no change which has been larger than the HV polarization image. The error area in HV polarization is very small while the error area in HH polarization is huge. Therefore, HV polarization images become easier to detect the deforested areas from natural forest areas than HH polarization images.

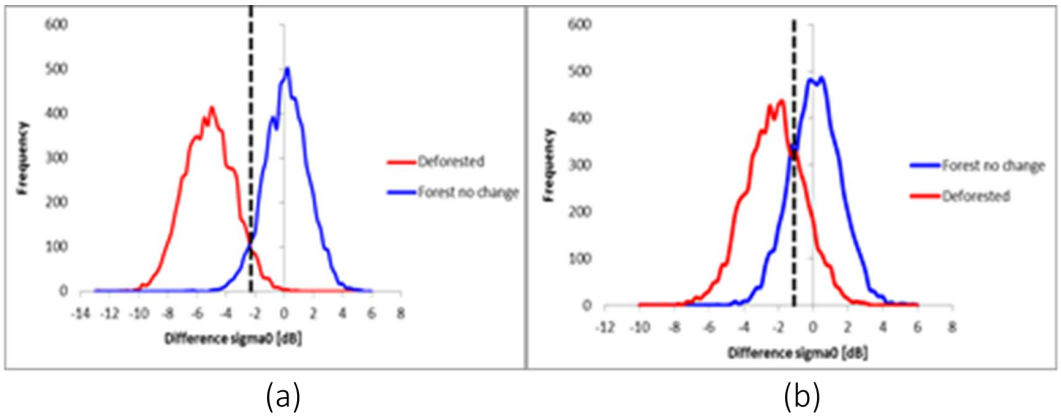

Figure 6. Histogram of difference σ^0 for deforested and forest no change, (a) HV polarization, (b) HH polarization

Capabilities of HV polarization on deforestation detection mapping is caused by the sensitivity of this signal to vertical objects such as tree trunk. Therefore the σ^0HV intensity will abruptly decrease after cutting the trees due to changes in the scattering mechanism. A decrease in σ^0HV is also caused by forest canopies that tend to depolarize the radar signal (random scattering: volume scattering), giving a solid HV signal that is lost when deforestation occurs.

3.2 The seasonal variation due to moisture effect on radar backscattering coefficient (σ^0)

Figure 7 shows the mean of σ^0HV values of bare soil in wet seasons that was larger than in dry seasons in both locations. The other land covers (settlement, forest, acacia, and oil palm) have no significant change during the wet and dry seasons. The low differences were in settlement and forest. In high accumulated rainfall, σ^0HV values increases significantly and decreases when the accumulated rainfall was in the lowest intensity, especially for bare soil.

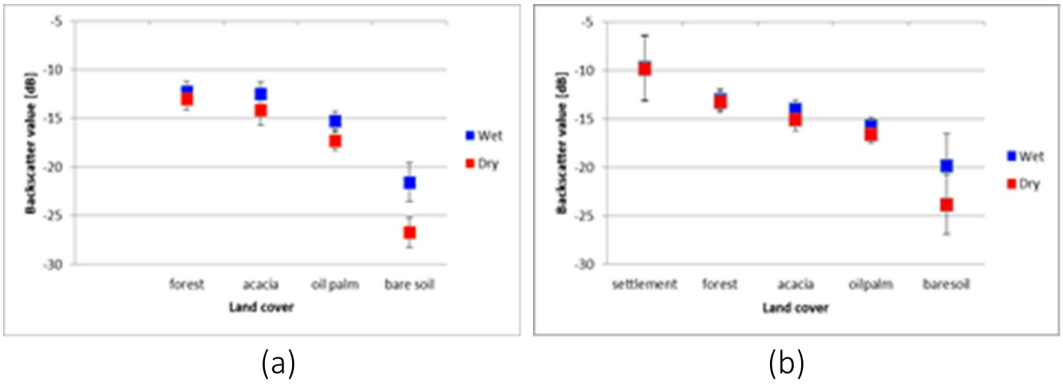

Figure 7. Seasonally averaged σ^0HV values for each land cover (a) in Borneo and (b) in Riau

Analysis of correlation is performed to investigate the correlation between σ^0HV intensity and accumulated rainfall for vegetation and bare soil.

According to Figure 8, the coefficient of correlation for the forest is the lowest among all of the vegetation classes (R= 0.374). The highest coefficient of determination was in bare soil (R= 0.702). The coefficient correlation of acacia and oil palm are 0.631 and 0.639.

The result shows that bare soil has the highest difference in dry and wet seasons. Moreover, there is a positive correlation between σ^0HV of bare soil (deforested areas) and accumulated rainfall. This phenomenon is caused by the amount of radar energy returned to the antenna (backscattering signal) depending on the dielectric constant of the target.

Heavy rainfall increased soil water content up to 85% at soil depths of 0-40 m (Xiu et al., 2011). Increasing the water content of targets will increase the dielectric constant. Based on the radar equation, the dielectric constant is proportional to the backscattering value. Otherwise, at a low concentration of water, most of the molecules bind to the grains, enabling the wave to penetrate the soil, then reducing the backscattering value.

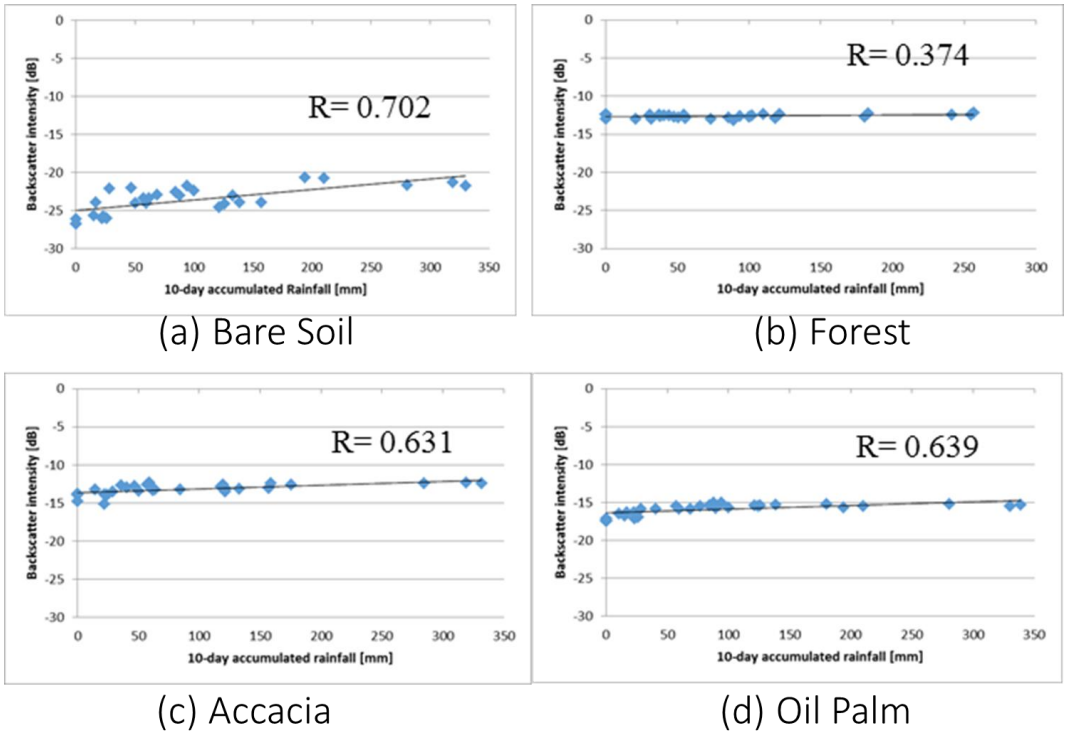

Figure 8. Correlation between backscatter intensity and accumulated rainfall for each land cover

3.3 Evaluation of seasonal variation's effect on deforestation detection

The σ^0HV difference between deforested areas and natural forests varies with time using FBD-1 (Figure 9). The σ^0HV differences between deforested areas and natural forests become small in particular time which can be seen in images acquired in September and October 2009. According to rainfall data from GsMap, the image acquisition time coincides with high accumulated rainfall (>90 mm/10-day).

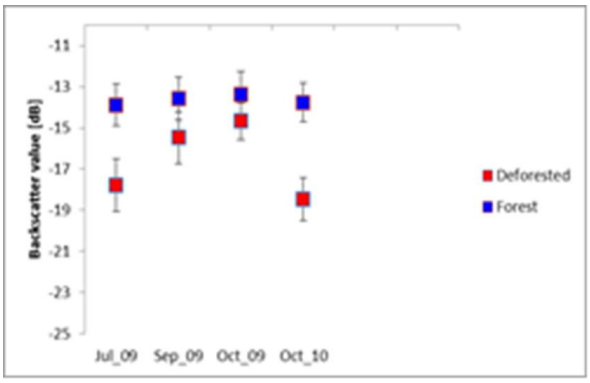

Figure 9. Time series of σ^0HV for natural forest and deforested areas in the FBD-1

Figure 10 shows the detection rate, false alarm rate, and accuracy rate of deforestation detection are obtained by using various thresholds for the different observation times of

σ^0HV. The relationship between the detection rate and thresholds is not always similar and it changes depending on the observation time. The detection rate is rapidly increasing at a threshold around -8 to -5 dB.

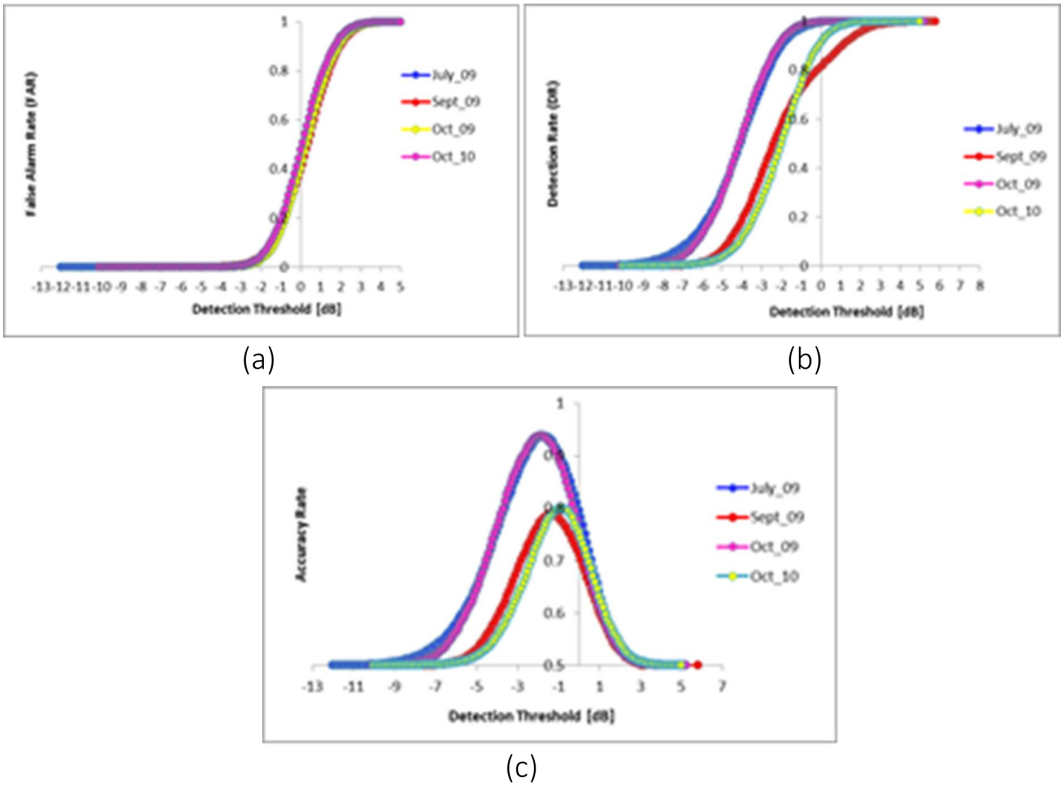

Figure 10. (a) False alarm rate, (b) detection rate, and (c)accuracy rate of different observation time

On the other hand, the false alarm rate for all data shows similar behavior and drasticly increase at a threshold of around -2.0 ~ -1.0 dB. The accuracy rate shows the maximum value when the threshold of the σ^0 difference is between -2 dB and -1dB. The maximum accuracy rate range from 79.05% to 93.84%. The maximum accuracy rate tend to decrease when the σ^0HV differences between deforested areas and natural forests were small, which is shown in Figure 9.

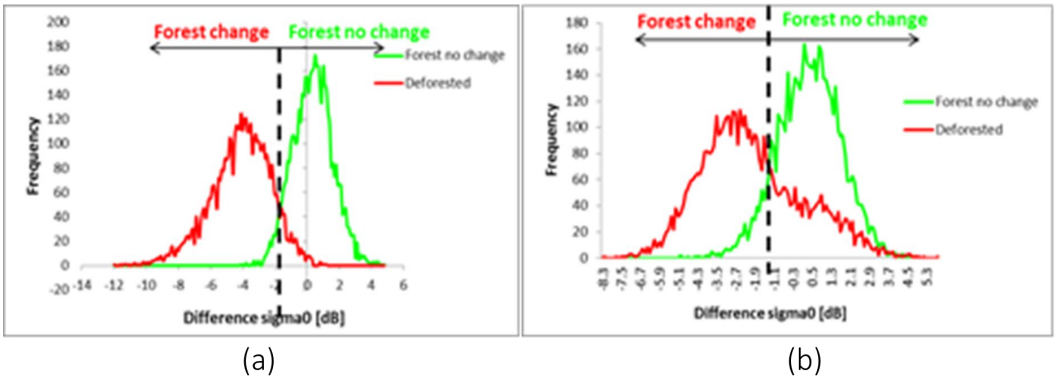

Figure 11. Histogram of difference $\sigma^0$for natural forest and deforested areas, (a) Image Nov/07-Oct/10 and (b) Image Nov/07-Oct/09

Figure 11 illustrates the histogram of difference σ^0 for deforested and forest no change areas. For image difference at Nov/07-Oct/09 which has a small difference σ^0 . In Figure 8, the numbers of pixels overlap between deforested and forests no change has been

larger than image difference at Nov/07-Oct/10 which has the large difference of σ^0. The error area in the difference image from Nov/07-Oct/09 is very small and the error area in the difference image from Nov/07-Oct/09 is considerably high. Therefore, the image difference which has a large difference of σ^0 between deforested and forest no change areas became easier to detect the deforested than the image which has a small difference of σ^0.

Based on data from Table 1, only two images have better accuracy rate (Nov_07-July_09 and Nov_07-October_10). Therefore, these images are chosen to make the deforestation map from 2009 to 2010.

Table 1. The accuracy rate of deforestation detection mapping using a threshold in FBD-1

Accumulated precipitation (mm/10-day)	Image difference	Maximum Accuracy Rate (%)	Threshold (dB)
0-89	Nov_07-Jul_09	93.76	-1.8
90<	Nov_07-Sep_09	79.05	-1.3
90<	Nov_07-Oct_09	79.94	-0.8
0-89	Nov_07-Oct_10	93.84	-1.8

The positive correlation between σ^0HV of bare soil (deforested areas) and accumulated rainfall can affect the accuracy rate of deforestation detection. In the high accumulated rainfall, the σ^0HV value of deforested areas increases and sometimes overlaps with the σ^0HV value of the natural forest. Therefore, the difference σ^0HV between deforested areas and natural forest becomes small and the accuracy rate of deforestation detection decrease. In the low accumulated rainfall, the σ^0HV value of deforested areas down significantly and the σ^0HV value of the natural forest is constant. Therefore the difference σ^0HV between deforested areas and natural forest become large. The deforested areas and natural forest are easy to distinguish. In this research, image observation time was selected in the dry season to reduce the error in the interpretation of deforestation detection.

3.4 Deforestation mapping

Figure 12 shows the deforestation map of FBD-1 in Riau with data period from November 2007 until October 2010 using HV polarization images and maximum threshold (-1.8 dB) based on the results described above. Deforestation areas from November 2007 to July 2009 were marked with red color, July 2009 to October 2010 marked with yellow color and the remain of forest cover area in October 2010 was marked in green color.

Table 2 explains the accuracy of the annual deforestation map assessed by using reference data from Global Forest Watch and a land use/cover map from the Indonesian Ministry of Forestry. The total pixels of “true” are 438 pixels and the overall accuracy of the mapping was 92.21%, which was almost the same as the accuracy rate obtained in the above-mentioned threshold evaluation.

The high accuracy of deforestation detection mapping using ALOS/PALSAR images is caused by several factors such as the high spatial resolution ALOS/PALSAR data that is 12.5 m x 12.5 m, the capability of SAR data to provide cloud-free images in tropical forest regions and the sensitivity of multi-polarization SAR data (co and cross-polarization) to detect the deforestation. The L band was representing a good classification of vegetation because the L-band has good penetration in vegetation areas.

Table 3 illustrates the total deforested areas are calculated by using PALSAR HV polarization data. Based on these data, the total deforested areas from November 2007 to

October 2010 is 22756.59 ha. The total forest cover area in November 2007 is 182910.712 ha. Forest areas in November 2007 reduce to 6.77 % in July 2009 and 6.08 % in October 2010.

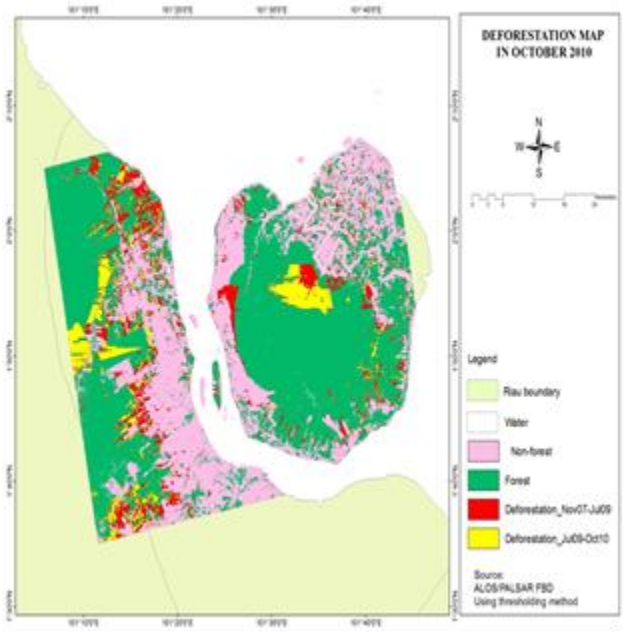

Figure 12. Deforestation map from November 2007 to October 2010 in Riau

Table 2. Confusion matrix for the yearly deforestation map obtained in FBD-1

		Reference data						User's Accuracy (%)
Detection By ALOS/PALSAR FBD		Water	Forest	Non-forest	Defo 2007-2009	Defo 2009-2010	Total	
	Water	42	0	0	0	1	43	97.67
	Forest	0	57	5	3	5	70	81.43
	Non-forest	3	8	72	2	1	86	83.72
	Defo 2007-2009	0	0	0	153	5	158	96.84
	Defo 2009-2010	0	0	0	4	114	118	96.61
	Total	45	65	77	162	126	475	
Producer's Accuracy (%)		93.33	87.69	93.51	94.44	90.48		92.21

Table 3. Forest covers loss in FBD-1, in Riau from 2009-2010

Month/Year	Forest cover loss area (ha)	Total Forest cover (ha)	Percentage forest covers loss (%)
Nov/07		182910.712	
N0v/07-Jul/09	15385.34	170525.372	6.77
Jul/09-Oct/10	10371.25	160154.122	6.08

The high rates of deforestation in Riau are due to clearing the natural forest cover to non-forest for industrial plantation (pulpwood and oil palm plantation). The WWF 2008 noted that the forest cover lost in the last 25 years, 24% was replaced by or cleared for

industrial pulpwood plantations, 29% was replaced by or cleared for industrial oil palm plantations and 17% became so-called "wasteland".

4. Conclusions

The accuracy rate of deforestation detection mapping using HV polarization provide better results than HH polarization. The better performance of HV polarization on deforestation detection mapping is caused by the sensitivity of this signal to vertical objects.

The seasonal change due to rainfall affect the radar backscattering signatures for bare soil, acacia, and oil palm, but not for forest areas. This phenomenon is caused by the positive correlation between σ^0HV of bare soil and accumulated rainfall.

The accuracy of the deforestation map based on the thresholding method is 92.21%. Forest areas in Riau in July 2007 reduce to 6.77 % in July 2009 and 6.08 % in October 2010.

Acknowledgments

I would like to say thanks to Japan Aerospace Exploration Agency (JAXA), which provided the ALOS/PALSAR data, and World Wide Fund (WWF) Indonesia which provided the ground truth data. I also appreciate the use of Global rainfall data from GSMap, forest cover loss map from Global Forest Watch (GFW), and Land use/cover map from the Indonesian Ministry of Forestry which can be downloaded freely. I would like to express my sincere gratitude to Prof. Kakuji Ogawara as a supervisor and Prof.Tasuku Tanaka as the Director of the Center for Remote Sensing and Ocean Science (CReSOS), Udayana University.

References

Hansen, M. C., Stehman, S. V., Potapov, P. V., Loveland, T. R., Townshend, J. R. G., DeFries, R. S., Pittman, K. W., Arunarwati, B., Stolle, F., Steininger, M. K., Carroll, M., & DiMiceli, C. (2008). *Humid tropical forest clearing from 2000 to 2005 was quantified by using multitemporal and multiresolution remotely sensed data*. In Proceedings of the National Academy of Sciences. Washington, DC, USA, 8 July 2008 (pp. 9439-9444).

Kiage, L. M., Walker, N. D., Balasubramanian, S., Babin, A., & Barras, J. (2005). Applications of Radarsat-1 synthetic aperture radar imagery to assess hurricane-related flooding of coastal Louisiana. *International Journal of Remote Sensing*, **26**(24), 5359-5380.

Margono, B. A., Turubanova, S., Zhuravleva, I., Potapov, P., Tyukavina, A., Baccini, A., Goetz, S., & Hansen, M. C. (2012). Mapping and monitoring deforestation and forest degradation in Sumatra (Indonesia) using Landsat time-series data sets from 1990 to 2010. *Environmental Research Letters*, **7**(3), 034010.

Motohka, T., Shimada, M., Uryu, Y., & Setiabudi, B. (2014). We are using time series PALSAR gamma naught mosaics for automatic detection of tropical deforestation: A test study in Riau, Indonesia. *Remote sensing of environment*, **155**, 79-88.

Salas, W. A., Ducey, M. J., Rignot, E., & Skole, D. (2002). Assessment of JERS-1 SAR for monitoring secondary vegetation in Amazonia: I. Spatial and temporal variability in backscatter across a chrono-sequence of secondary vegetation stands in Rondonia. *International Journal of Remote Sensing*, **23**(7), 1357-1379.

Shimada, M., Isoguchi, O., Tadono, T., & Isono, K. (2009). PALSAR radiometric and geometric calibration. *IEEE Transactions on Geoscience and Remote Sensing*, **47**(12), 3915-3932.

Thiel, C., Drezet, P., Weise, C., Quegan, S., & Schmullius, C. (2006). Radar remote sensing for the delineation of forest cover maps and the detection of deforestation. *Forestry*, **79**(5), 589-597.

Tsuyuki, S., Goh, M. H., Teo, S., Kamlun, K. U., & Phua, M. H. (2011). Monitoring deforestation in Sarawak, Malaysia using multitemporal Landsat data. *Kanto Forest Research*, **62**, 87-90.

Whittle, M., Quegan, S., Uryu, Y., Stüewe, M., & Yulianto, K. (2012). Detection of tropical deforestation using ALOS-PALSAR: A Sumatran case study. *Remote Sensing of Environment*, **124**, 83-98.

WWF Indonesia. (2009). *Deforestation Forest Degradation Biodiversity Loss and CO2 Emissions in Riau Sumatra Indonesia*. Jakarta, Indonesia: WWF Indonesia. World Wide Fund for Nature Indonesia.

Xu, Q., Liu, S., Wan, X., Jiang, C., Song, X., & Wang, J. (2012). Effects of rainfall on soil moisture and water movement in a subalpine dark coniferous forest in southwestern China. *Hydrological Processes*, **26**(25), 3800-3809.
